Ultrastructural and Immunohistochemical Study on the Lamina Propria Cells Beneath Paneth Cells in the Rat Ileum

Mantani, Youhei ; Nishida, Miho ; Yamamoto, Kyouji ; Miyamoto, Kazuki ; Yuasa, Hideto ; Masuda, Natsumi ; Omotehara, Takuya ; Tsuruta, Hiroki …

(Citation)
Anatomical Record: Advances in Integrative Anatomy and Evolutionary Biology,301(6):1074-1085

(Issue Date)
2018-01

(Resource Type)
journal article

(Version)
Accepted Manuscript

(URL)
https://hdl.handle.net/20.500.14094/90006214

Ultrastructural and immunohistochemical study on the lamina propria cells beneath Paneth cells in the rat ileum

Youhei MANTANI[1)], Miho NISHIDA[1)], Kyouji YAMAMOTO[1)], Kazuki MIYAMOTO[1)], Hideto YUASA[1)], Natsumi MASUDA[1)], Takuya OMOTEHARA[2)], Hiroki TSURUTA[3, 4)], Toshifumi YOKOYAMA[5)], Nobuhiko HOSHI[5)] and Hiroshi KITAGAWA[1)]

[1)] *Laboratory of Histophysiology, Department of Bioresource Science, Graduate School of Agricultural Science, Kobe University, 1-1 Rokkodai-cho, Nada-ku, Kobe, Hyogo 657-8501, Japan*

[2)] *Department of Anatomy, Tokyo Medical University, 6-1-1 Shinjuku, Shinjuku-ku, Tokyo 160-8042, Japan*

[3)] *Center for Collaborative Research and Technology Development, Kobe University, 1-1 Rokkodai-cho, Nada-ku, Kobe, Hyogo 657-8501, Japan*

[4)] *Research Unit for Future Creation & Innovation "Creative Dojo", Graduate School of Engineering, Kobe University, 1-1 Rokkodai-cho, Nada-ku, Kobe, Hyogo 657-8501, Japan*

[5)] *Laboratory of Animal Molecular Morphology, Department of Bioresource Science, Graduate School of Agricultural Science, Kobe University, 1-1 Rokkodai-cho, Nada-ku, Kobe, Hyogo 657-8501, Japan*

Running title: Lamina propria cells beneath Paneth cells

Correspondence: MANTANI, Y., Laboratory of Histophysiology, Graduate School of Agricultural Science, Kobe University, 1-1 Rokkodai-cho, Nada-ku, Kobe, Hyogo 657-8501, Japan. Tel.: +81-78-803-6586. e-mail: mantani@sapphire.kobe-u.ac.jp

Grant sponsor: Japan Society for the Promotion of Science; Grant numbers: 15K07766 and 16K18813.

ABSTRACT

Paneth cells secrete bactericidal substances in response to bacterial proliferation on the mucosal surface without directly contacting bacteria. However, the induction mechanism of this transient secretion has not been clarified, although nervous system and/or immunocompetent cells in the lamina propria (LP) might be involved. In the present study, we ultrastructurally and immunohistochemically investigated which LP cells are localized beneath Paneth cells and examined the relationship between the Paneth cell-derived cellular processes which extended into the LP and the LP cells. The results showed that various cells, including blood capillary, subepithelial stromal cell and nerve fiber, were present in the LP beneath Paneth cells. Endothelial cells of blood capillary were the cells most frequently found in this location; they were situated within 1 μm of the Paneth cells and possessed fenestration on the surfaces adjacent to Paneth cells. The Paneth cells rarely extended the cellular processes toward the LP across the basal lamina. Most of the cellular processes of Paneth cells contacted the subepithelial stromal cells. Immunohistochemistry revealed that the $CD34^{+}CD31^{-}\alpha SMA^{-}$ stromal cells preferentially localized in the LP beneath the intestinal crypt base, while $PDGFR\alpha^{hi}\alpha SMA^{+}$ stromal cells mainly localized around the lateral portions of the intestinal crypt and $PDGFR\alpha^{hi}\alpha SMA^{-}$ stromal cells localized in the intestinal villus. From these findings, the existence of blood capillaries beneath Paneth cells might reflect the active exocrine function of Paneth cells. Furthermore, subepithelial stromal cells, probably with a $CD34^{+}CD31^{-}\alpha SMA^{-}PDGFR\alpha^{-/lo}$ phenotype, beneath the crypt base might affect Paneth cell activity by interacting with their cellular processes.

Key words: Ileum; Paneth cell; rat; transmission electron microscopy

INTRODUCTION

Numerous indigenous bacteria settle in the alimentary tract of animals. This bacterial settlement is initiated immediately after birth by bacteria derived from the mother, and the number and composition of indigenous bacteria are stable in the adult alimentary tract (Batt et al., 1996). The settlement of indigenous bacteria is regulated by various factors from their hosts, including rapid migration of epithelial cells, acceleration of epithelial cell proliferation, physical elimination by epithelial cells, digestive enzymes, bactericidal peptides, and so on (Inamoto et al., 2008a, b; Mantani et al., 2013; Qi et al., 2009a, b; Yokoo et al., 2011a, b). Lysozyme, soluble phospholipase A2 (sPLA2), α-defensin, and β-defensin-1 and -2 have all been proposed to regulate the settlement of indigenous bacteria in the animal alimentary tract (Salzman et al., 2010; Yokoo et al., 2011a, b). In the small intestine, Paneth cells play an important role in the regulation of indigenous bacteria with bactericidal substances contained in the secretory granules. Accordingly, the loss of Paneth cells leads to an increase of bacterial translocation from the intestines and consequent inflammation (Grootjans et al., 2011). Among the above bactericidal substances, lysozyme and sPLA2 are secreted from Paneth cells in the rat ileum in response to hyperproliferation of indigenous bacteria in the intervillous spaces without direct contact between indigenous bacteria and Paneth cells (Yokoo et al., 2011a). This bacterial proliferation in the intervillous spaces might be monitored by Toll-like receptor-2 expressed on the villous columnar epithelial cells throughout the rat small intestine (Mantani et al., 2011). However, the manner by which bacterial stimulation from the villous columnar epithelial cells is delivered to Paneth cells has not been clarified.

Paneth cells have been shown to secrete secretory substances in response to various stimulations in an experimental setting. For example, exposure of intestinal crypts isolated from the mouse small intestine to bacteria or lipopolysaccharide (LPS) induces the secretion of α-defensin from Paneth cells (Ayabe et al., 2000). Injection of LPS into the lumen of the rat small intestine also leads to sPLA2-secretion from Paneth cells (Qu et al., 1996). Peroral administration of bacteria-derived CpG-DNA, flagellin or LPS induces transient secretion from Paneth cells in mice (Rumio et al., 2012). In addition to these bacterial components, IFN-γ derived from immunocompetent cells and carbamylcholine induce transient secretion from Paneth cells in mouse small intestinal organoids (Farin et al., 2014). Furthermore, several cholinergic agents, including carbamylcholine and bethanechol, induce transient secretion from mouse Paneth cells *in vivo* (Satoh et al., 1992; Satoh et al., 1989). From these findings, it is hypothesized that bacterial stimulation from the intestinal lumen can be delivered to Paneth cells and induce the transient secretion from Paneth cells *via* some pathway, such as the nervous system and/or immunocompetent cells, in the lamina propria. To determine which system is the most likely candidate for the induction of transient secretion from Paneth cells, histological components in the lamina propria beneath Paneth cells should be fully examined. Therefore, the primary aim of this study was to investigate which lamina propria cells are localized beneath Paneth cells, using both ultrastructural analysis and immunohistochemistry. Furthermore, Paneth cells in the rat small intestine are known to extend their cellular processes into the lamina propria (Behnke and Moe, 1964), suggesting that the cellular processes from Paneth cells might be equipped to communicate with the lamina propria

cells. However, the significance of these cellular processes has not been clarified. Therefore, the secondary aim of this study was to examine the relationship between the cellular processes from Paneth cells and the lamina propria cells beneath Paneth cells.

MATERIALS AND METHODS

Animals

Fourteen male Wistar rats aged 7 weeks (Japan SLC Inc., Hamamatsu, Shizuoka, Japan) were maintained under specific pathogen-free conditions in individual ventilated cages (Sealsafe Plus; Tecniplast S.p.A, Buguggiate, Italy) with controlled temperature (23 ± 1°C) and humidity (50%) on a 12/12 or 14/10-hr light/dark cycle at the Kobe University Life-Science Laboratory. They were permitted free access to water and food (Lab RA-2; Nosan Corp., Yokohama, Kanagawa, Japan). Clinical and pathological examinations in all animals confirmed that there were no signs of disorder. This experiment was approved by the Institutional Animal Care and Use Committee (permission number: 25-06-01) and carried out according to the Kobe University Animal Experimentation Regulations.

Electron microscopy

After euthanasia by overdose peritoneal injection of pentobarbital sodium (Kyoritsu Seiyaku Corp., Tokyo, Japan), small tissue blocks were removed from the ilea of 9 rats, and immersion-fixed in 2.5% glutaraldehyde and 2.0% paraformaldehyde fixative in 0.1 M phosphate buffer (PB; pH 7.4) for 24 hr at 4ºC. After postfixation with 1.0% OsO_4 in PB for 90 min at room temperature

(r.t.), the small specimens were dehydrated and embedded in a Quetol 812 mixture. Ultrathin sections of approximately 70 nm thickness were cut using an ultramicrotome (Sorvall MT-1: Dupont, Newton, CT) and stained with both 4% uranyl acetate solution and lead citrate solutions by the method of Sato with modifications by Hanaichi (1986). The ultrathin sections were observed under an H-7100 (Hitachi, Tokyo, Japan) or JEM-1400 (JEOL Ltd, Tokyo, Japan) transmission electron microscope at an accelerating voltage of 75 or 80 kV.

Tissue preparation for light microscopy

After euthanasia by overdose peritoneal injection of pentobarbital sodium (Kyoritsu Seiyaku Corp.), tissue blocks were removed from the ilea of 5 rats. Then, half of each tissue block was immersed in OCT compound (Sakura Finetek Japan Co. Ltd., Tokyo, Japan) and snap-frozen in liquid nitrogen for the detection of CD34 and CD31, and the other half of each block was immersion-fixed in 4.0% paraformaldehyde fixative in PB for 6 hr at 4ºC, then snap-frozen in liquid nitrogen as described previously (Mantani et al., 2014) for the detection of CD34, α-SMA and PDGFRα. Sections were cut at a thickness of 5 or 4 μm using a Coldtome Leica CM1950 (Leica Biosystems, Nuβloch, Germany) and placed on slide glasses precoated with 0.2% 3-aminopropyltriethoxysilane (Shin-Etsu Chemical Co., Tokyo, Japan), and stored at -30ºC until use.

Enzyme immunohistochemistry and double immunofluorescence method

Antigens were detected using the indirect method of immunohistochemistry. Briefly, the unfixed sections for the detection of both CD34 and CD31 were

fixed with 10% formalin for 10 min and rinsed with 0.05% Tween-added 0.01 M phosphate-buffered saline (TPBS; pH 7.4), whereas the pre-fixed sections for the detection of CD34, α-SMA and PDGFRα were rinsed with TPBS. All sections were then immersed in absolute methanol and 0.5% H_2O_2 for 30 min, respectively. The sections were rinsed three times in TPBS after each preparation step to remove any reagent residues. Following blocking with Blocking One Histo (Nacalai Tesque Inc., Kyoto, Japan) for 1 hr at r.t., the sections to be used for the enzyme immunohistochemical analysis were reacted with anti-rat CD34 goat IgG (diluted at 1:800, AF-4117; R&D Systems Inc., Minneapolis, MN, USA), anti-rat CD31 mouse IgG (diluted at 1:50, NB100-64796SS; Novus Biologicals LLC., Littleton, CO, USA), anti-human α-SMA mouse IgG (diluted at 1:400, ab7817; Abcam, Cambridge, MA, USA) and anti-mouse PDGFRα goat IgG (diluted at 1:3,200, AF-1062; R&D Systems Inc.) for 18 hr at 6 ºC. The sections for the immunofluorescence analysis (except for the section for immunofluorescence against CD34/PDGFRα) were reacted with one of three pairings—anti-rat CD34 goat IgG (diluted at 1:800)/anti-rat CD31 mouse IgG (diluted at 1:50), anti-rat CD34 goat IgG (diluted at 1:800)/anti-human α-SMA mouse IgG (diluted at 1:400) or anti-mouse PDGFRα goat IgG (diluted at 1:800)/anti-human α-SMA mouse IgG (diluted at 1:400) —for 18 hr at 6 ºC. The sections for immunofluorescence against CD34/PDGFRα were first reacted with anti-rat CD34 goat IgG (diluted at 1:800) for 18 hr at 6 ºC.

Next, the sections for the enzyme immunohistochemical analysis were incubated with horseradish peroxidase (HRP)-conjugated anti-goat IgG donkey IgG (diluted at 1:200, 705-035-147; Jackson ImmunoResearch Inc., West Grove,

PA, USA) or HRP-conjugated anti-mouse IgG rat IgG (diluted at 1:200, 415-035-166; Jackson ImmunoResearch Inc.) for 1 hr at r.t. They were then incubated with 3,3'-diaminobenzidine (Dojindo Lab., Mashiki, Kumamoto, Japan) containing 0.03% H_2O_2 and counterstained with hematoxylin. For immunofluorescence for the detection of CD34/CD31, CD34/α-SMA and PDGFRα/α-SMA, the sections were reacted with Alexa 488-conjugated anti-goat IgG donkey IgG (diluted at 1:400 or 1,600, ab150133; Abcam), Alexa 568-conjugated anti-mouse IgG donkey IgG (diluted at 1:400 or 1,600, ab175700; Abcam), and DAPI (diluted at 1:1,000; Dojindo Lab.) for 1 hr at r.t. The sections for immunofluorescence against CD34/PDGFRα were reacted with Alexa 568-conjugated anti-goat IgG donkey IgG (diluted at 1:3,200, ab175704; Abcam) and DAPI (diluted at 1:1,000; Dojindo Lab.), then blocked with normal goat IgG (500-G00) (diluted at 1:100; Peprotech Inc., Rocky Hill, NJ, USA) for 1 hr at r.t., and finally reacted with Alexa 488-conjugated anti-PDGFRα goat IgG (diluted at 1:10, FAB-1062G; R&D Systems Inc.), which is equivalent to Alexa 488-conjugated anti-PDGFRα goat IgG (AF-1062), for 18 hr at 6 ºC. Sections for the enzyme immunohistochemical analysis were then observed under the light microscope, while those for immunofluorescence analysis were observed under the fluorescent microscope. Control sections were incubated with TPBS or non-immunized goat or mouse IgG instead of the primary antibody.

Western blotting

Whether or not the anti-mouse PDGFRα goat IgG (AF-1062; R&D Systems Inc.) used in the above immunohistochemical analysis possesses cross reactivity

against rat PDGFRα was examined with western blotting using rat PDGFRα recombinant protein (80433-R08H; Sino Biological Inc., Beijing, China), because this cross reactivity was not ensured by the manufacturer. Briefly, 0.25 ng of rat PDGFRα was reduced at 95 ºC for 5 min with sample buffer containing sodium dodecyl sulfate (SDS), separated by SDS/PAGE and transferred onto a polyvinylidene difluoride membrane. Following blocking with Blocking One (Nacalai Tesque Inc.) for 1 hr at r.t., the membrane was reacted with anti-mouse PDGFRα goat IgG (diluted at 1:10,000, AF-1062; R&D Systems Inc.) for 18 hr at 6 ºC and with HRP-conjugated anti-goat IgG donkey IgG (diluted at 1:10,000, 705-035-147; Jackson ImmunoResearch Inc.) for 1 hr at r.t. Finally, the immunoreactive band was visualized using Chemi-Lumi One Super (Nacalai Tesque Inc.) and Amersham hyperfilm ECL (GE Healthcare, Amersham Place, Buckinghamshire, UK).

Histoplanimetry and statistical analysis

Distinct stromal cells possessing moniliform cellular processes have been reported to exist around the intestinal crypt in the rat duodenum (Carmona et al., 2011) and jejunum (Cretoiu et al., 2012). Therefore, the territory of the stromal cells with moniliform cellular processes was investigated in the rat ileum. Under a transmission electron microscope, twenty photos containing lamina propria of at least 80 μm^2 were taken from each of four mucosal portions as shown in Fig. 1. Then, the length of the stromal cell-derived moniliform cellular process per unit area was calculated for each photo. Statistical analysis was performed with the Kruskal Wallis test with Steel-Dwass as a posthoc analysis for comparisons among the four portions. *P* values less than 0.05

were considered statistically significant.

RESULTS

Ultrastructural observation of the lamina propria beneath Paneth cells

In the lamina propria beneath Paneth cells, blood capillaries, pericytes, subepithelial stromal cells and nerve fibers were found, with the blood capillary being the most prevalent. Migrating cells, such as eosinophils, plasma cells and macrophage-like cells, the latter of which possessed numerous lysosomes, were also found in the lamina propria near the intestinal crypt base rather than beneath Paneth cells.

Blood capillaries were frequently and closely localized beneath Paneth cells. Endothelial cells of blood capillary cells possessed fenestration on the surfaces adjacent to Paneth cells. On the other hand, blood capillaries in the lamina propria around the lateral portions of the intestinal crypt did not possess fenestration and were slightly separated from the basal lamina beneath the epithelium. Blood capillaries beneath Paneth cells were localized within 1 μm of Paneth cells, whereas those in the lamina propria around the lateral portions of the intestinal crypt were not found within 1 μm of the epithelium (Fig. 2). Pericytes extended their cellular processes across the basal lamina of the blood capillaries and surrounded the endothelial cells.

The subepithelial stromal cells in the lamina propria around the crypt base possessed long cellular processes, and an oval or triangular nucleus rich in euchromatin and organelles such as rough endoplasmic reticulum and mitochondria (Fig. 3a). The occupancy rate of the nucleus in the cytoplasm was high, while organelles in the cytoplasm were scarce. Cellular processes

from the subepithelial stromal cells frequently contained some organelles, rough endoplasmic reticulum which was occasionally swollen into a spherical form, and mitochondria, and therefore had a moniliform aspect (Fig. 3b, c). The subepithelial stromal cells or moniliform cellular processes rarely contacted eosinophils, plasma cells or smooth muscle cells in the lamina propria (Fig. 3d-g). The frequency of appearance of the moniliform cellular processes was significantly higher in the lamina propria around the intestinal crypt bases than in the lamina propria in other portions (Fig. 3h).

Paneth cells rarely extended their cellular process toward the lamina propria across the basal lamina. Most cellular processes of Paneth cells came into contact with the subepithelial stromal cells or thin cellular processes from stromal cells, while contacts with the blood capillaries, pericytes, migrating cells and nerve fibers were never found (Fig. 4). No secretory granules or vesicles of any size were found in the cellular processes from Paneth cells. Cellular process across basal lamina was never found in the undifferentiated columnar epithelial cells adjacent to Paneth cells.

Nerve fibers in the lamina propria beneath the intestinal crypt base were observed as a bundle of unmyelinated fibers (Fig. 4a), whereas discrete, individual nerve fibers were not detected. Nerve bundles never directly contacted the Paneth cells, although secretory vesicles were found in each nerve fiber.

Immunohistochemical phenotype of subepithelial stromal cells in the lamina propria around the intestinal crypt

Next, the phenotypes of subepithelial stromal cells in the lamina propria

around the intestinal crypt were investigated, because subepithelial stromal cells were speculated to have a spatial relationship with Paneth cells based on the above transmission electron microscopy. PDGFRα was immunohistochemically detected in the subepithelial stromal cells localizing in the lamina propria from the villous apex to the intestinal crypt base with an anti-mouse PDGFRα antibody that was confirmed to have specificity for rat PDGFRα by western blotting (Fig. 5a). PDGFRα^{+} stromal cells were frequently found from the apical portion of the intestinal villus to the lateral portion of the intestinal crypt, but were less frequent beneath the intestinal crypt base than in the other portions (Fig. 5b, c). In addition, PDGFRα-strongly-positive (PDGFRα^{hi}) stromal cells were found beneath the epithelium from the apical portion of the intestinal villus to the intestinal crypt base, while PDGFRα-weakly-positive (PDGFRα^{lo}) stromal cells were additionally found beneath the epithelium in the intestinal crypt base (Fig. 5c).

αSMA, a marker for myofibroblasts which are the most representative subepithelial stromal cells, was detected in the subepithelial stromal cells around the intestinal crypt. αSMA^{+} subepithelial stromal cells were more frequent in the lateral portions than in the basal portions of the intestinal crypts. In the intestinal villi, αSMA was detected in the villous myocytes. On the other hand, αSMA^{+} subepithelial stromal cells were rarely detected in the basal portions of intestinal villi, and were not detected at all in the middle to apical portions of intestinal villi (Fig. 6a, b). Double immunofluorescence against αSMA and PDGFRα revealed that PDGFRα^{hi} subepithelial stromal cells from the intestinal crypt bases to the basal portions of intestinal villi were immunopositive for αSMA. PDGFRα^{hi} subepithelial stromal cells from the middle to apical

portions in the intestinal villi were negative for αSMA (Fig. 7a-f). PDGFRα^{hi}αSMA^{-} subepithelial stromal cells were never found around the intestinal crypt. PDGFRα^{lo}αSMA^{-} subepithelial stromal cells were hardly found in the lamina propria around the intestinal crypt.

CD34 was detected in the stromal cells localizing in the lamina propria beneath the intestinal crypt bases, and in the endothelial cells of blood capillaries in the whole mucosa (Fig. 8a-c). CD31, an endothelial cell marker, was detected in the cell membrane of the endothelial cells of a blood capillary and of a lymphatic vessel, but not in other cells in the lamina propria (Fig. 8d-f). Double immunofluorescence against CD34 and CD31 confirmed that CD34^{+}CD31^{-} stromal cells were mainly localized in the lamina propria beneath the intestinal crypt base, whereas all CD34^{+}cells in the intestinal villus were positive for CD31 (Fig. 9). Moreover, double immunopositivity against CD34 and αSMA was never found in the ileal mucosa (Fig. 10). CD34^{+} stromal cells around the intestinal crypt bases were negative for PDGFRα. The PDGFRα^{hi} stromal cells that were frequently localized around the lateral portions of the intestinal crypts were negative for CD34 (Fig. 11).

DISCUSSION

Various exocrine glands, such as the salivary glands (Mohamed, 1975; Suddick and Dowd, 1969), prostate (Shabsigh et al., 1999), pancreas (Egerbacher and Böck, 1997), sweat glands (Quick et al., 1984) and Harderian glands (Strum and Shear, 1982), possess a well-developed blood capillary network with fenestrations in endothelial cells. Accordingly, several reports have suggested the importance of blood supply for exocrine function. For

example, a reduction of salivary flow has been shown to coincide with impaired blood flow in the submandibular gland of nonobese diabetic mice after muscarinic receptor activation (Berggreen et al., 2009). Moreover, a reduction of blood capillaries leads to a reduction of salivary flow in the salivary glands of irradiated mice (Cotrim et al., 2007). Thus, an extensive capillary network with fenestration is considered to function to supply the fluids required for exocrine function in the exocrine glands (Suddick and Dowd, 1969). The blood capillary-network is also well developed in the lamina propria of the intestinal crypt base in the rat small intestine (Ohashi et al., 1976). In the present study, blood capillaries whose endothelial cells exhibited fenestration on their surfaces adjacent to Paneth cells were frequently and closely localized beneath Paneth cells. From these findings, the blood capillary-network beneath Paneth cells might reflect the active exocrine function of Paneth cells. Exocytosis is found in Paneth cells of non-stimulated rats (Behnke and Moe, 1964), although secretions from Paneth cells are accelerated by bacteria (Satoh and Vollrath, 1986; Yokoo et al., 2011a), bacterial constituents (Qu et al., 1996; Rumio et al., 2012), neurotransmitters (Satoh et al., 1992) and cytokines (Farin et al., 2014). These findings suggest that there are two types of secretion in Paneth cells: homeostatic secretion and transient secretion in large quantities. A well-developed blood capillary network probably exists in order to supply the fluids required for the secretions.

Paneth cells in the rat small intestine extend their cellular processes into the lamina propria (Behnke and Moe, 1964), although the significance of this fact has not been clarified. In the present study, as in the report of Behnke and Moe (1964), the Paneth cell-derived cellular processes extended into the lamina

propria and directly contacted stromal cells in the lamina propria. Intestinal subepithelial stromal cells are known to contribute to the maintenance of intestinal homeostasis *via* various factors, such as Wnt signaling, which is essential for the maintenance of undifferentiated stem cells in the crypt (Fevr et al., 2007), or bone morphogenetic protein antagonists such as gremlin 1, gremlin 2, chordin-like 1 (Kosinski et al., 2007) and noggin (He et al., 2004), while the manner of communication between epithelial cells and subepithelial stromal cells is ambiguous. The direct contact between Paneth cells and stromal cells observed in the present study might thus represent a novel method of communication between these cells. In addition, the Paneth cells in the present study never possessed any vesicles in their cellular processes, which suggests that cellular processes of Paneth cells probably contribute to the reception of information, rather than its transmission. Based on these findings, subepithelial stromal cells beneath the crypt base might be able to affect the activity of Paneth cells *via* the cellular processes. Further investigations will be needed to clarify the functional significance of the cellular processes from Paneth cells and whether or not other types of epithelial cells possess similar cellular processes.

Subepithelial stromal cells have been referred to as subepithelial mesenchymal cells or subepithelial fibroblasts and are known to form the reticular structure beneath the epithelium. The stromal cells in the small intestine contain some subtypes showing different phenotypes, such as αSMA^+ myofibroblasts (human: Powell et al., 2011; mouse: Stzepourginski et al., 2017), $PDGFR\alpha^+$ cells (mouse: Iino et al., 2009) and $CD34^+gp38^+$ mesenchymal cells (mouse: Stzepourginski et al., 2017), although the relationships among these

subtypes have not been fully clarified. In the present study, we examined the phenotypes of subepithelial stromal cells in the rat ileum and their relationship. Our results suggested that subepithelial stromal cells in the rat ileum could be subdivided into three subtypes by immunohistochemistry: PDGFRα^{+}αSMA^{-}CD34^{-} cells in the intestinal villus, PDGFRα^{hi}αSMA^{+}CD34^{-} cells (myofibroblasts) mainly localizing in the lateral portions of the intestinal crypt and CD34^{+}CD31^{-}αSMA^{-} cells in the crypt base. PDGFRα was not detected in CD34^{+} cells around the crypt base in the double immunofluorescence, but PDGFRα^{lo} subepithelial stromal cells were found in the intestinal crypt base in enzyme immunohistochemistry, suggesting that the CD34^{+}CD31^{-}αSMA^{-} cells may have been PDGFRα^{lo} cells (see the schema in Fig. 12). From these findings, specific stromal cells exhibiting the CD34^{+}CD31^{-}αSMA^{-}PDGFRα$^{-/lo}$ phenotype were suggested to exist beneath Paneth cells localizing in the intestinal crypt base of the rat ileum, in agreement with a report in mice by Stzepourginski et al. (2017). Moreover, a distinctive type of stromal cells, telocytes, has been reported around the intestinal crypt in the rat duodenum and jejunum using a transmission electron microscope (Carmona et al., 2011; Cretoiu et al., 2012). Telocytes are ultrastructurally defined as stromal cells that possess a distinctive moniliform cellular process called a telopode, which is composed of two repeating parts: expanded parts and extremely thin parts (Cretoiu and Popescu 2014). In the present study, subepithelial cells showing the above ultrastructural characteristics were found, especially around the intestinal crypt base. Moreover, direct contacts between Paneth cells and distinctive moniliform cellular processes were also found. From these findings, subepithelial stromal cells that contact Paneth cells were suggested to

correspond to $CD34^{+}gp38^{+}$ cells as reported by Stzepourginski et al. (2017) or to telocytes as reported by Cretoiu et al. (2012). $CD34^{+}gp38^{+}$ cells construct a specialized microenvironment that maintains intestinal epithelial stem cells in the intestinal crypt base (Stzepourginski et al., 2017). Considering the findings in the present study, the stromal cells around the intestinal crypt base might contribute to the activity of Paneth cells, not only intestinal epithelial stem cells. In the future, the functional relationship between subepithelial stromal cells and Paneth cells should be investigated.

LITERATURE CITED

Ayabe T, Satchell DP, Wilson CL, Parks WC, Selsted ME, Ouellette AJ. 2000. Secretion of microbicidal α-defensins by intestinal Paneth cells in response to bacteria. Nat Immunol 1: 113-118.

Batt RM, Rutgers HC, Sancak AA. 1996. Enteric bacteria: friend or foe? J Small Anim Pract 37: 261-267.

Behnke O, Moe H. 1964. An electron microscope study of mature and differentiating Paneth cells in the rat, especially of their endoplasmic reticulum and lysosomes. J Cell Biol 22: 633-652.

Berggreen E, Nyløkken K, Delaleu N, Hajdaragic-Ibricevic H, Jonsson MV. 2009. Impaired vascular responses to parasympathetic nerve stimulation and muscarinic receptor activation in the submandibular gland in nonobese diabetic mice. Arthritis Res Ther 11: R18.

Carmona IC, Bartolomé MJL, Escribano CJ. 2011. Identification of telocytes in the lamina propria of rat duodenum: transmission electron microscopy. J Cell Mol Med 15: 26-30.

Cotrim AP, Sowers A, Mitchell JB, Baum BJ. 2007. Prevention of irradiation-induced salivary hypofunction by microvessel protection in mouse salivary glands. Mol Ther 15: 2101-2106.

Cretoiu D, Cretoiu SM, Simionescu AA, Popescu LM. 2012. Telocytes, a distinct type of cell among the stromal cells present in the lamina propria of jejunum. Histol Histopathol 27: 1067-1078.

Cretoiu D, Popescu LM. 2014. Telocyte revisited. Biomol Concepts 5: 353-369.

Egerbacher M, Böck P. 1997. Morphology of the pancreatic duct system in mammals. Microsc Res Tech 37: 407-417.

444 Farin HF, Karthaus WR, Kujala P, Rakhshandehroo M, Schwank G, Vries RGJ,
445 Kalkhoven E, Nieuwenhuis EES, Clevers H. 2014. Paneth cell extrusion and
446 release of antimicrobial products is directly controlled by immune
447 cell-derived IFN-γ. J Exp Med 211: 1393-1405.
448 Fevr T, Robine S, Louvard D, Huelsken J. 2007. Wnt/β-catenin is essential for
449 intestinal homeostasis and maintenance of intestinal stem cells. Mol Cell Biol
450 27:7551-7559.
451 Grootjans J, Hodin CM, De Haan J-J, Derikx JPM, Rouschop KMA, Verheyen
452 FK, Van Dam RM, Dejong CHC, Buurman WA, Lenaerts K. 2011. Level of
453 activation of the unfolded protein response correlates with Paneth cell
454 apoptosis in human small intestine exposed to ischemia/reperfusion.
455 Gastroenterol 140, 529-539.
456 Hanaichi T, Sato T, Iwamoto T, Malavasi-Yamashiro J, Hoshino M, Mizuno N.
457 1986. A stable lead by modification of Sato's method. J Electron Microsc 35:
458 304-306.
459 He XC, Zhang J, Tong W-G, Tawfik O, Ross J, Scoville DH, Tian Q, Zheng X,
460 He X, Wiedemann LM, Mishina Y, Li L. 2004. BMP signaling inhibits
461 intestinal stem cell self-renewal through suppression of Wnt–β-catenin
462 signaling. Nat Genet 36: 1117-1121.
463 Iino S, Horiguchi K, Horiguchi S, Nojyo Y. 2009. c-Kit-negative fibroblast-like
464 cells express platelet-derived growth factor receptor α in the murine
465 gastrointestinal musculature. Histochem Cell Biol 131: 691-702.
466 Inamoto T, Kawata Y, Qi W-M, Yamamoto K, Warita K, Kawano J, Yokoyama T,
467 Hoshi N, Kitagawa H. 2008a. Ultrastructural study on the epithelial responses
468 against attachment of indigenous bacteria to epithelial membranes in Peyer's

patches of rat small intestine. J Vet Med Sci 70: 235-241.

Inamoto T, Namba M, Qi W-M, Yamamoto K, Yokoo Y, Miyata H, Kawano J, Yokoyama T, Hoshi N, Kitagawa H. 2008b. An immunohistochemical detection of actin and myosin in the indigenous bacteria-adhering sites of microvillous columnar epithelial cells in Peyer's patches and intestinal villi in the rat jejunoileum. J Vet Med Sci 70: 1153-1158.

Kosinski C, Li VSW, Chan ASY, Zhang J, Ho C, Tsui WY, Chan TL, Mifflin RC, Powell DW, Yuen ST, Leung SY, Chen X. 2007. Gene expression patterns of human colon tops and basal crypts and BMP antagonists as intestinal stem cell niche factors. Proc Natl Acad Sci U S A 104: 15418-15423.

Mantani Y, Kamezaki A, Udayanga KGS, Takahara E, Qi W-M, Kawano J, Yokoyama T, Hoshi N, Kitagawa H. 2011. Site differences of Toll-like receptor expression in the mucous epithelium of rat small intestine. Histol Histopathol 26, 1295-1303.

Mantani Y, Nishida M, Yuasa H, Yamamoto K, Takahara E, Omotehara T, Udayanga KGS, Kawano J, Yokoyama T, Hoshi N, Kitagawa H. 2014. Ultrastructural and histochemical study on the Paneth cells in the rat ascending colon. Anat Rec 297: 1462-1471.

Mantani Y, Takahara E, Takeuchi T, Kawano J, Yokoyama T, Hoshi N, Kitagawa H. 2013. Histoplanimetrical study on the relationship between invasion of indigenous bacteria into intestinal crypts and proliferation of epithelial cells in rat ascending colon. J Vet Med Sci 75: 939-947.

Mohamed AH. 1975. Ultrastructural permeability studies in capillaries of rabbit oral mucosa and salivary glands. Microvasc Res 9: 287-303.

Ohashi Y, Kita S, Murakami T. 1976. Microcirculation of the rat small intestine

494 as studied by the injection replica scanning electron microscope method. Arch
495 Histol Jpn 39: 271-282.
496 Powell DW, Pinchuk IV, Saada JI, Chen X, Mifflin RC. 2011. Mesenchymal
497 cells of the intestinal lamina propria. Annu Rev Physiol 73: 213-237.
498 Qi W-M, Yamamoto K, Yokoo Y, Miyata H, Inamoto T, Udayanga KGS,
499 Kawano J, Yokoyama T, Hoshi N, Kitagawa H. 2009a. Histoplanimetrical
500 study on the relationship between the cell kinetics of villous columnar
501 epithelial cells and the proliferation of indigenous bacteria in rat small
502 intestine. J Vet Med Sci 71: 463-470.
503 Qi W-M, Yamamoto K, Yokoo Y, Miyata H, Udayanga KGS, Kawano J,
504 Yokoyama T, Hoshi N, Kitagawa H. 2009b. Histoplanimetrical study on the
505 relationship between cellular kinetics of epithelial cells and proliferation of
506 indigenous bacteria in the rat colon. J Vet Med Sci 71: 745-752.
507 Qu X-D, Lloyd KCK, Walsh JH, Lehrer RI. 1996. Secretion of type II
508 phospholipase A2 and cryptdin by rat small intestinal Paneth cells. Infect
509 Immun 64: 5161-5165.
510 Quick DC, Kennedy WR, Yoon KS. 1984. Ultrastructure of the secretory
511 epithelium, nerve fibers, and capillaries in the mouse sweat gland. Anat Rec
512 208: 491-499.
513 Rumio C, Sommariva M, Sfondrini L, Palazzo M, Morelli D, Viganò L, De
514 Cecco L, Tagliabue E, Balsari A. 2012. Induction of Paneth cell degranulation
515 by orally administered Toll-like receptor ligands. J Cell Physiol 227:
516 1107-1113.
517 Salzman NH, Hung K, Haribhai D, Chu H, Karlsson-Sjöberg J, Amir E, Teggatz
518 P, Barman M, Hayward M, Eastwood D, Stoel M, Zhou Y, Sodergren E,

519 Weinstock GM, Bevins CL, Williams CB, Bos NA. 2010. Enteric defensins
520 are essential regulators of intestinal microbial ecology. Nat Immunol 11:
521 76-83.
522 Satoh Y, Ishikawa K, Oomori Y, Takeda S, Ono K. 1992. Bethanechol and a
523 G-protein activator, NaF/AlCl3, induce secretory response in Paneth cells of
524 mouse intestine. Cell Tissue Res 269: 213-220.
525 Satoh Y, Ishikawa K, Oomori Y, Yamano M, Ono K. 1989. Effects of
526 cholecystokinin and carbamylcholine on Paneth cell secretion in mice: a
527 comparison with pancreatic acinar cells. Anat Rec 225: 124-132.
528 Satoh Y, Vollrath L. 1986. Quantitative electron microscopic observations on
529 Paneth cells of germfree and ex-germfree Wistar rats. Anat Embryol 173:
530 317-322.
531 Shabsigh A, Tanji N, D'agati V, Burchardt T, Burchardt M, Hayek O, Shabsigh
532 R, Buttyan R. 1999. Vascular anatomy of the rat ventral prostate. Anat Rec
533 256: 403-411.
534 Strum JM, Shear CR. 1982. Harderian glands in mice: fluorescence, peroxidase
535 activity and fine structure. Tissue Cell 14: 135-148.
536 Stzepourginski I, Nigro G, Jacob JM, Dulauroy S, Sansonetti PJ, Eberl G,
537 Peduto L. 2017. CD34+ mesenchymal cells are a major component of the
538 intestinal stem cells niche at homeostasis and after injury. Proc Natl Acad Sci
539 U S A 114: E506-E513.
540 Suddick RP, Dowd FJ. 1969. The microvascular architecture of the rat
541 submaxillary gland: possible relationship to secretory mechanisms. Arch Oral
542 Biol 14: 567-576.
543 Yokoo Y, Miyata H, Udayanga KGS, Qi W-M, Takahara E, Mantani Y,

544 Yokoyama T, Kawano J, Hoshi N, Kitagawa H. 2011a. Immunohistochemical
545 and histoplanimetrical study on the spatial relationship between the settlement
546 of indigenous bacteria and the secretion of bactericidal peptides in rat
547 alimentary tract. J Vet Med Sci 73: 1043-1050.
548 Yokoo Y, Miyata H, Udayanga KGS, Qi W-M, Takahara E, Yokoyama T,
549 Kawano J, Hoshi N, Kitagawa H. 2011b. Immunohistochemical study on the
550 secretory host defense system of bactericidal peptides in rat digestive organs.
551 J Vet Med Sci 73: 217-225.
552

553 **FIGURE LEGENDS**

554 Fig. 1. Histoplanimetrically measured areas: 1) apical portion of the intestinal
555 villus (IV), 2) basal portion of the IV, 3) lateral portion of the intestinal crypt
556 (IC) and 4) basal portion of the IC.

557

558 Fig. 2. Ultrastructure of blood capillaries in the lamina propria beneath a
559 Paneth cell (a, b) and around the lateral portion of the intestinal crypt (c). a)
560 Blood capillaries (BC) are visible just beneath the Paneth cell (PC). Bar = 10
561 μm. b) High magnification image of the BC beneath PC. The endothelial cell
562 of the BC shows fenestration on the surfaces adjacent to PC (arrows). Bar =
563 200 nm. c) BC in the lamina propria around the lateral portion of the intestinal
564 crypt is visible separately from the epithelium (EC). L, lymphatic vessel. Bar
565 = 1 μm.

566

567 Fig. 3. a-c) Ultrastructure of subepithelial stromal cells in the lamina propria
568 around the intestinal crypt base. a) A subepithelial stromal cell (arrow)
569 possesses scarce cytoplasm, a triangular nucleus, and an extremely thin cellular
570 process (black arrowheads). In the cellular process and cytoplasm, spherically
571 expanded rough endoplasmic reticula are observed (red arrowheads). Bar = 1
572 μm. b) Typical ultrastructural image of a moniliform cellular process in the
573 lamina propria around the intestinal crypt base. The moniliform cellular
574 process is long and extremely thin cellular processes and are composed of two
575 repeating parts: expanded parts (arrows) and extremely thin parts (arrowheads).
576 EP, epithelium. Bar = 1 μm. c) High-magnification image of a moniliform
577 cellular process in the rectangular area in 3b. The expanded part (along the red

line) containing the expanded rough endoplasmic reticula (asterisks) and the extremely thin part (along the blue line) containing no organelles are clearly visible. The rough endoplasmic reticula (asterisks) found in the moniliform cellular process are spherically expanded. Bar = 1 μm. d-f) Contact between a subepithelial stromal cell (arrow) and a smooth muscle cell (e, arrowhead) or an eosinophil (f, arrowhead). e) High magnification image of the square area with a black line in 3d. f) High magnification image of the square area with a blue line in 3d. g) Contact between a moniliform cellular process (arrows) and plasma cell. Eo, eosinophil. SC, stromal cell. SM, smooth muscle cell. PL, plasma cell. Bar = 1 μm. h) Histoplanimetrical results of the distribution of moniliform cellular processes in the four portions indicated in Fig. 1. Asterisk, $P<0.05$. Double asterisks, $P<0.01$.

Fig. 4. Contact between the cellular processes (black asterisks) of Paneth cells and subepithelial stromal cells (a) or thin cellular process (b, c) (arrowheads). The cellular process contacting Paneth cells (b) possesses spherically extended rough endoplasmic reticulum (blue asterisks). c) High magnification image of the black rectangular area in 4b. Nerve fibers (a, arrow) are visible near the stromal cells. BM, basal membrane. PC, Paneth cell. a) Bar = 1 μm. b, c) Bar = 200 nm.

Fig. 5. Localization of PDGFRα in the rat ileal mucosa. a) Recombinant rat PDGFRα (70-110 kDa) is detected using anti-mouse PDGFRα goat antibody (AF-1062) by western blotting. b-c) Strongly PDGFRα-immunopositive stromal cells (arrows) are visible beneath the epithelial cells in the intestinal

603 villus (b) and the lateral portions of the intestinal crypt (c), while weakly
604 PDGFRα-immunopositive ones are visible beneath the intestinal crypt base (c,
605 arrowheads). Bar = 10 μm.
606
607 Fig. 6. Immunohistochemical localization of αSMA in the intestinal villus (a)
608 and intestinal crypt (b). a) αSMA-immunopositivity is visible in the villous
609 myocytes (arrows). b) An αSMA-immunopositive stromal cell is visible
610 beneath the epithelial cells in the lateral portions of the intestinal crypt (arrow).
611 Bar = 10 μm.
612
613 Fig. 7. Double immunofluorescence against PDGFRα (green) and αSMA (red).
614 a-c) In the lamina propria of the intestinal villus, co-localization of PDGFRα and
615 αSMA is not visible, although PDGFRα^{+} subepithelial stromal cells are visible
616 (white arrows). d-f) PDGFRα^{+} subepithelial stromal cells around the intestinal
617 crypt are positive for αSMA (yellow arrows). Bar = 10 μm.
618
619 Fig. 8. Localization of CD34 (a-c) and CD31 (d-f) in the rat ileal mucosa. a)
620 CD34-immunopositivity is observed in the subepithelial region of the lamina
621 propria in intestinal villi and around crypts. Bar = 100 μm. b, c)
622 High-magnification image of the apical portion of the intestinal villus (b) and
623 around the intestinal crypt (c). In the intestinal villus, CD34-immunopositivity
624 is visible in the subepithelial endothelial cells of blood capillaries in the lamina
625 propria but not in the other tissue components (b). c) CD34-immunopositivity
626 is visible in the extremely thin subepithelial stromal cells (arrows), not only in
627 the endothelial cells of blood capillaries in the lamina propria beneath the

intestinal crypt. Blue line, border between the lamina propria and muscularis mucosae. d) CD31-immunopositivity in the lamina propria is visible in the subepithelial region from the intestinal villus to the intestinal crypt (arrows) and the central region of the intestinal villus (arrowheads). Bar = 100 μm. e, f) High-magnification image of the apical portion of the intestinal villus (e) and around the intestinal crypt (f). CD31-immunopositivity is visible in the cell membrane of endothelial cells in the blood capillaries in the intestinal villus (e) and beneath the intestinal crypt (f). Bar = 10 μm.

Fig. 9. Double immunofluorescence against CD34 (green) and CD31 (red). a-c) In the lamina propria of the intestinal villus, $CD34^{+}CD31^{+}$ endothelial cells of blood capillaries are visible in the subepithelial regions (yellow arrows), whereas $CD34^{-}CD31^{+}$ endothelial cells of lymphoid vessels are visible in the central regions (white arrowheads). $CD34^{+}CD31^{-}$ cells are not visible. d-f) In the lamina propria beneath the intestinal crypt base, $CD34^{+}CD31^{-}$ stromal cells (white arrows) are visible as well as $CD34^{+}CD31^{+}$ endothelial cells of blood capillaries (yellow arrows). Bar = 10 μm.

Fig. 10. Double immunofluorescence against CD34 (green) and αSMA (red). In the lamina propria of the intestinal villus (a) and around the intestinal crypt (b), co-localization of CD34 and αSMA is not visible. A $CD34^{+}$ stromal cell is visible beneath the epithelial cells in the base of the intestinal crypt (arrow), whereas an $αSMA^{+}$ stromal cell is visible beneath the epithelial cells in the lateral portion of the intestinal crypt (arrowhead). MM, muscularis mucosae. SM, submucosal layer. Bar = 10 μm.

Fig. 11. Double immunofluorescence against PDGFRα (green) and CD34 (red). A $CD34^+$ stromal cell is visible beneath the epithelial cells in the base of the intestinal crypt (white arrows) and is negative for PDGFRα, whereas $PDGFR\alpha^+$ cells are visible beneath the epithelial cells in the lateral portion of the intestinal crypt (white arrowheads) and are negative for CD34. Bar = 10 μm.

Fig. 12. Schema of the distribution of subepithelial stromal cells in the rat ileum. Dashed line, crypt orifice.

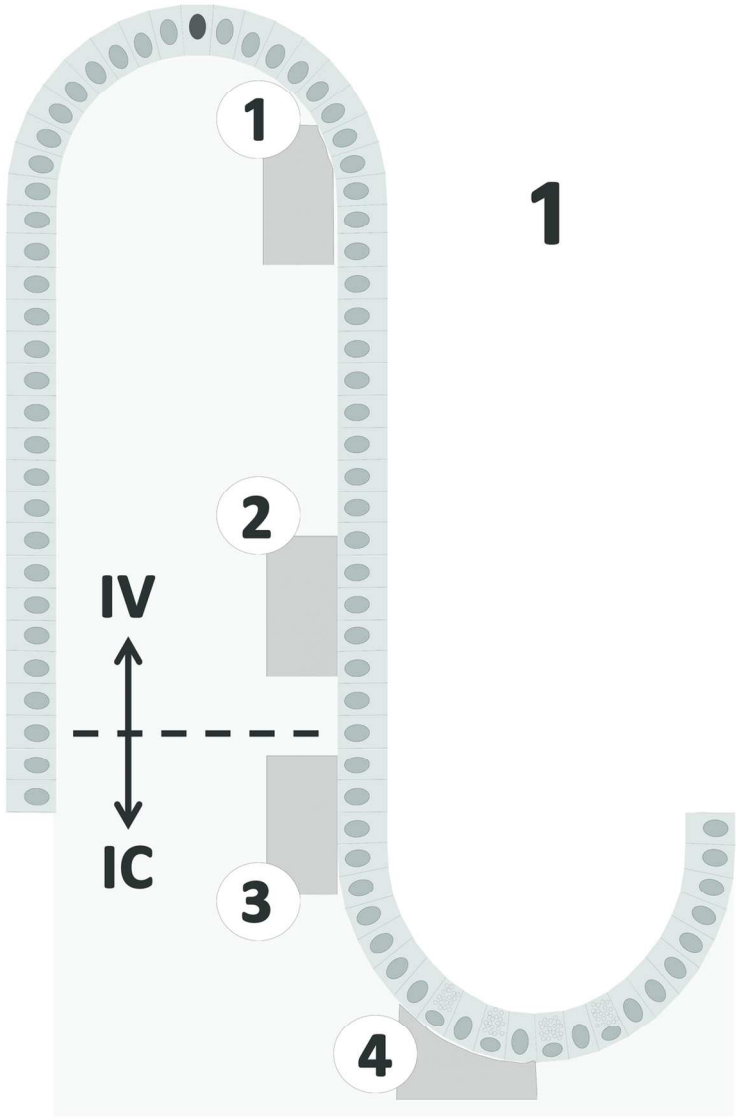

Fig. 1. Histoplanimetrically measured areas: 1) apical portion of the intestinal villus (IV), 2) basal portion of the IV, 3) lateral portion of the intestinal crypt (IC) and 4) basal portion of the IC.

52x84mm (600 x 600 DPI)

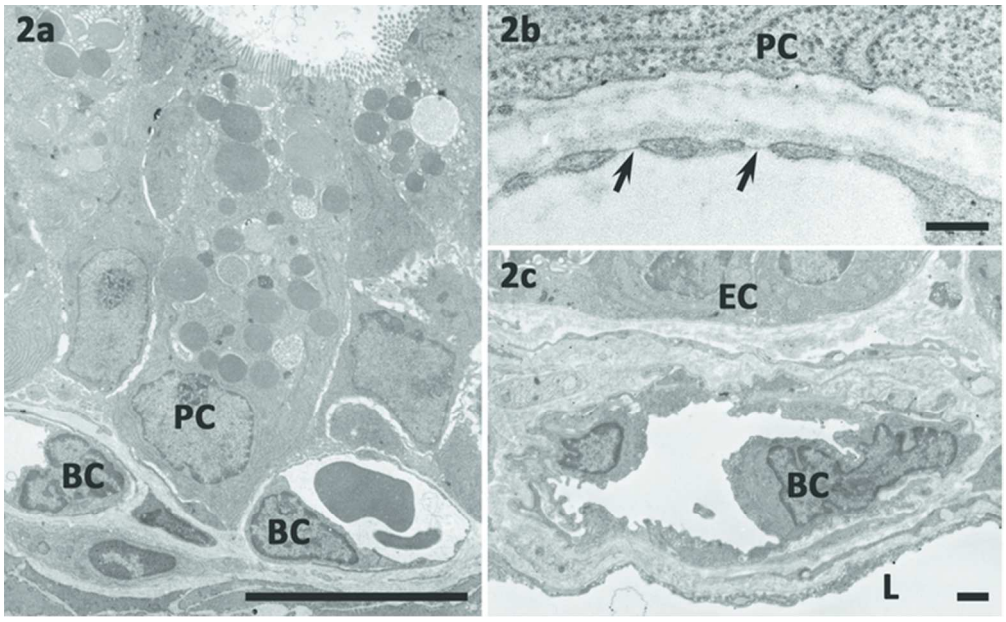

Fig. 2. Ultrastructure of blood capillaries in the lamina propria beneath a Paneth cell (a, b) and around the lateral portion of the intestinal crypt (c).

64x39mm (300 x 300 DPI)

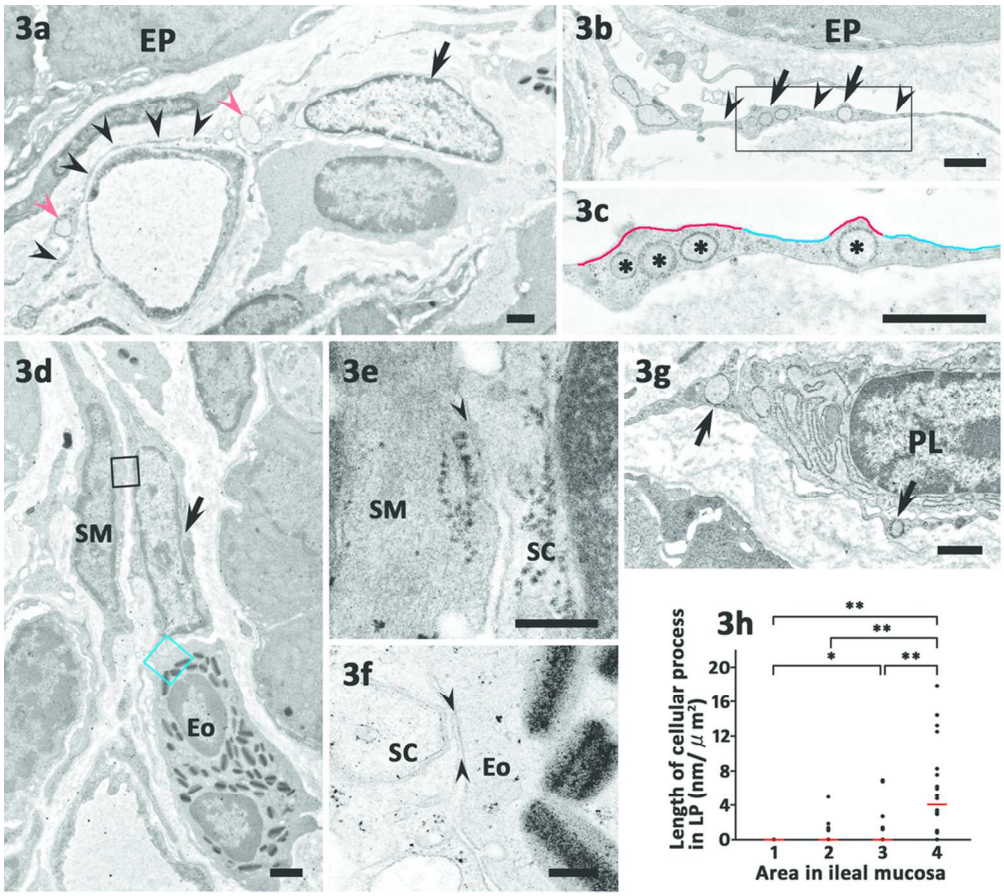

Fig. 3. Ultrastructure of subepithelial stromal cells in the lamina propria around the intestinal crypt base.

93x83mm (300 x 300 DPI)

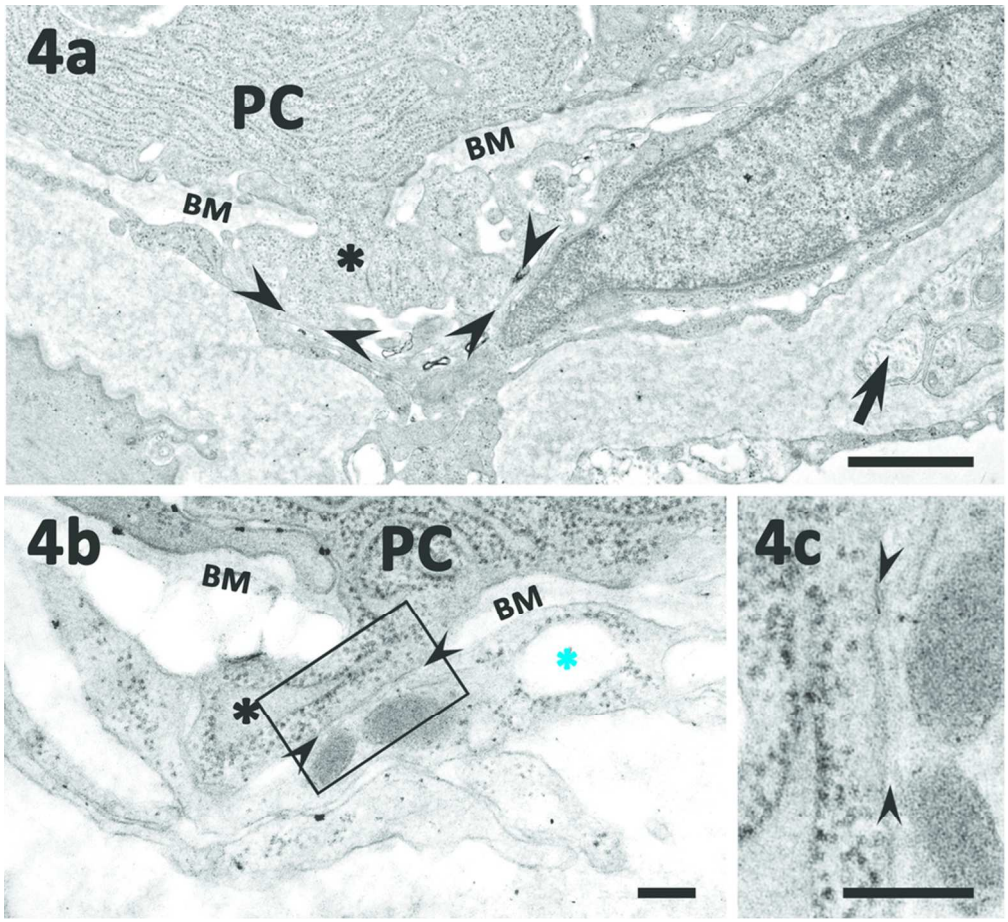

Contact between the cellular processes (black asterisks) of Paneth cells and subepithelial stromal cells (a) or thin cellular process (b, c) (arrowheads).

85x78mm (300 x 300 DPI)

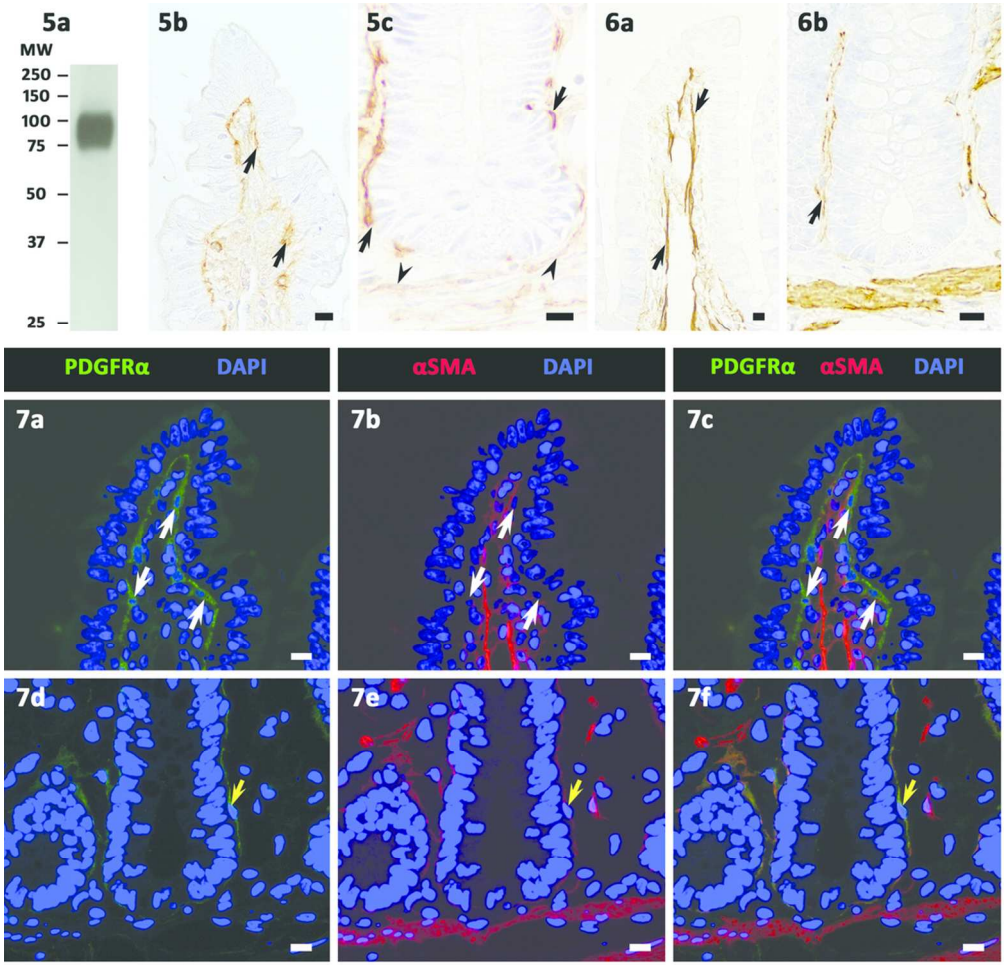

Fig. 5. Localization of PDGFRα in the intestinal villus (b) and intestinal crypt (b).
Fig. 6. Immunohistochemical localization of αSMA in the intestinal villus (a) and intestinal crypt (b).
Fig. 7. Double immunofluorescence against PDGFRα (green) and αSMA (red) in the intestinal villus (a-c) and intestinal crypt (d-f).

101x97mm (300 x 300 DPI)

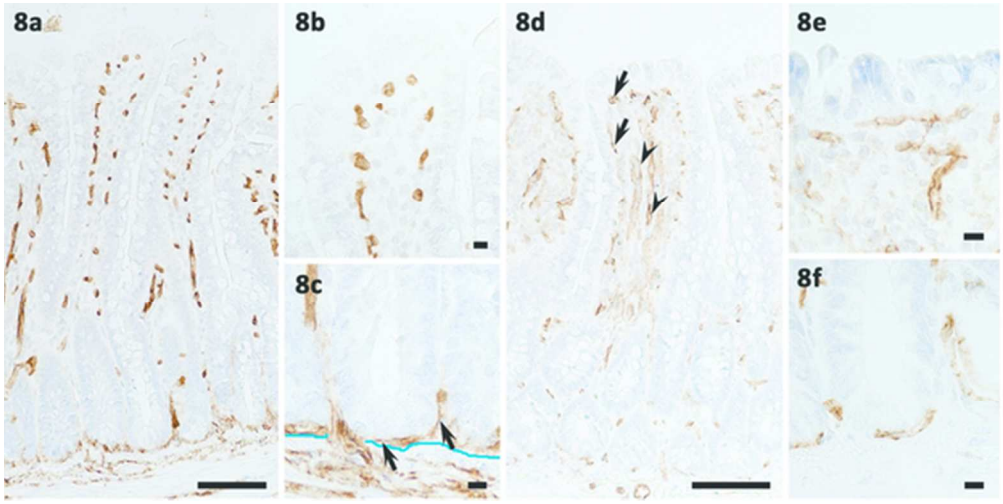

Fig. 8. Localization of CD34 (a-c) and CD31 (d-f) in the rat ileal mucosa.

52x26mm (300 x 300 DPI)

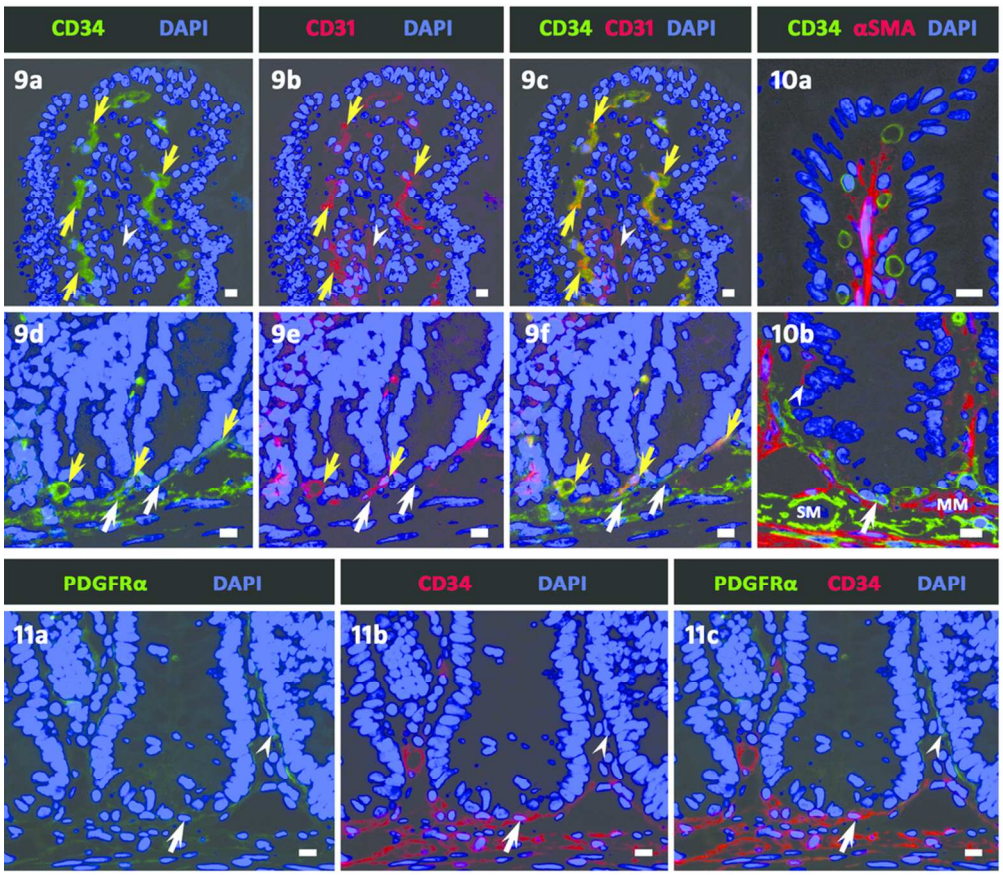

Fig. 9. Double immunofluorescence against CD34 (green) and CD31 (red) in the intestinal villus (a-c) and intestinal crypt (d-f).
Fig. 10. Double immunofluorescence against CD34 (green) and αSMA (red) in the intestinal villus (a) and intestinal crypt (d).
Fig. 11. Double immunofluorescence against PDGFRα (green) and CD34 (red) in the intestinal crypt.

92x80mm (300 x 300 DPI)

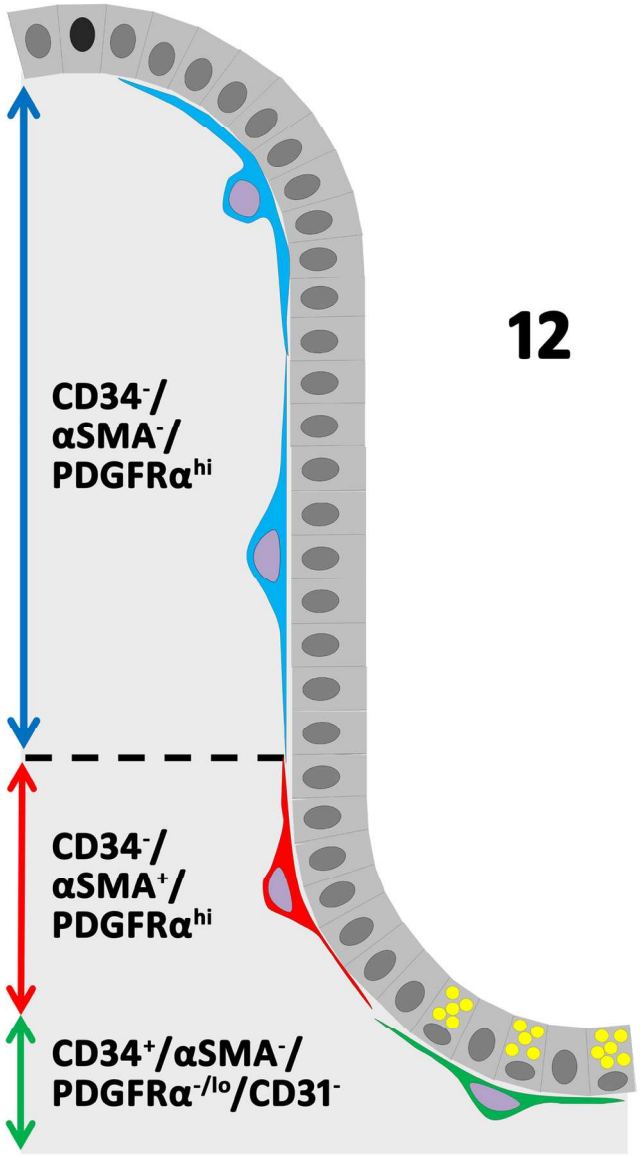

Schema of the distribution of subepithelial stromal cells in the rat ileum. Dashed line, crypt orifice.

52x94mm (600 x 600 DPI)